PLASMA DYNAMICS

XIII. PLASMAS AND CONTROLLED NUCLEAR FUSION*

A. Waves and Radiation

Academic and Research Staff

Prof. G. Bekefi
Prof. W. P. Allis
Prof. A. Bers
Prof. S. C. Brown
Prof. B. Coppi
Prof. E. V. George
Prof. R. J. Taylor
Dr. P. A. Politzer
Dr. D. J. Sigmar
Dr. A. Treves
J. J. McCarthy
W. J. Mulligan

Graduate Students

H. Bhattacharya
F. W. Chambers
D. Prosnitz
M. L. Vianna

RESEARCH OBJECTIVES

We continue our experimental and theoretical program designed to gain further understanding of the various types of waves and oscillations in ionized gases. We are particularly interested in processes that are relevant to controlled thermonuclear fusion and space research.

One of our major goals is the study of waves and radiation of large amplitude under conditions where nonlinear phenomena and plasma turbulence are prominent. In this connection we are studying such problems as the nonlinear coupling of two or more electromagnetic waves and anomalous absorption of intense microwave and laser radiation by the plasma. Studies of turbulence and fluctuations in plasma confined in two-dimensional magnetic field configurations are contemplated. For this purpose we shall use our steady-state linear quadrupole (SLIM-1) and our small toroidal facility (MINITOR). The construction of these two machines has been recently completed.

G. Bekefi

1. BREMSSTRAHLUNG INSTABILITY IN A PLASMA, INDUCED BY ELECTRON STREAMING

Introduction

It is known that collisions between plasma particles can stimulate unstable electromagnetic oscillations within the ionized medium.[1] This class of instabilities requires, in addition to a non-Maxwellian velocity distribution, a collision rate depending strongly on the particle energy.[2] These requirements can be shown to bear some resemblance to those necessary for the occurrence of maser action in quantum devices. For that reason, collision-induced plasma instabilities have usually been treated quantum-mechanically.

*This work was supported by the U. S. Atomic Energy Commission (Contract AT(11-1)-3070).

Calculations[3] indicate that collisions of electrons with neutral atoms in Ramsauer-like gases (e.g., argon, xenon, krypton) have a particularly favorable energy dependence for exciting instabilities. Experiments[4] made both in the absence and presence of an external dc magnetic field tend to confirm the theoretical predictions. A problem of more general interest concerns the role of these instabilities in highly ionized media where Coulomb encounters dominate. The problem may have relevance for astronomical plasmas,[5] and in the production and heating of plasmas by means of lasers[6] and radio waves.[7] As early as 1958, Twiss[8] addressed himself to this question of stability. Using a semiclassical description of the emission and absorption processes, he argued that electron-ion impacts can never lead to negative absorption (instability), however widely the energy distribution in the electron gas may diverge from that of thermal equilibrium. This conclusion seems to be diametrically opposed by more recent work of Marcuse,[9] and of Bunkin and Fedorov[10] who, on the basis of a full quantum-mechanical model, find that under certain conditions negative absorption may indeed be possible.

In this report we show that both views are correct: an isotropic distribution of electron velocities (assumed implicitly by Twiss), however non-Maxwellian it may be, cannot lead to a collisional instability in an electron-ion plasma. On the other hand, if the distribution function is sufficiently anisotropic as in the case of the monoenergetic electron stream postulated by Marcuse, the system can, in fact, become unstable.

In our treatment the dispersion equation for transverse electromagnetic waves propagating in the plasma is derived from the classical, nonrelativistic Boltzmann equation. Particle collisions are allowed for by means of the familiar but approximate "relaxation" model containing a speed-dependent collision rate. The special case of a monoenergetic electron beam interacting with a background of ions is examined at length, and a detailed stability analysis is carried out. The analysis shows that for plasma parameters of practical interest, the waves are absolutely unstable and the instability is confined to a narrow range of frequencies near, but above, the electron plasma frequency. In the limit of a very tenuous plasma where collective effects can be disregarded, we recover the results obtained by Marcuse.

Dispersion Relation

We describe the perturbation of the plasma electrons caused by an electromagnetic wave, through the linearized Boltzmann equation,

$$\frac{\partial f_1}{\partial t} + \underset{\sim}{v} \cdot \frac{\partial f_1}{\partial \underset{\sim}{r}} - \frac{e}{m}\left[\underset{\sim}{E}_o + \underset{\sim}{v} \times \underset{\sim}{B}_o\right] \cdot \frac{\partial f_1}{\partial \underset{\sim}{v}} - \frac{e}{m}\left[\underset{\sim}{E}_1 + \underset{\sim}{v} \times \underset{\sim}{B}_1\right] \cdot \frac{\partial f}{\partial \underset{\sim}{v}} = -\nu(v)\, f_1. \tag{1}$$

Here $f(\underset{\sim}{v})$ is the distribution of electron velocities in the absence of the perturbation; it is assumed to be known. The parameter $f_1(\mathbf{v}, \mathbf{r}, t)$ is a small perturbation caused by the electromagnetic wave with RF fields given by $\mathbf{E}_1$ and $\mathbf{B}_1$; $\mathbf{E}_o$ and $\mathbf{B}_o$ represent the equilibrium fields. The right-hand side of the equation is an approximation to the Boltzmann collision integral with $\nu(v)$ as the speed-dependent collision frequency for momentum transfer.

When we assume that there are no static $\mathbf{E}_o$ and $\mathbf{B}_o$ fields and that the electron motions are nonrelativistic, we find from Eq. 1 that

$$\frac{\partial f_1}{\partial t} + \mathbf{v} \cdot \frac{\partial f_1}{\partial \mathbf{r}} - \frac{e}{m} \mathbf{E}_1 \cdot \frac{\partial f}{\partial \mathbf{v}} = -\nu(v)\, f_1. \tag{2}$$

Allowing all oscillatory quantities contained in Eq. 2 to vary as $\exp[j\omega t - j\mathbf{k} \cdot \mathbf{r}]$, we solve for f_1 with the result that

$$f_1 = \frac{e}{m} \frac{\mathbf{E}_1 \cdot (\partial f/\partial \mathbf{v})}{j\omega - j\mathbf{k} \cdot \mathbf{v} + \nu(v)}. \tag{3}$$

We find that the transverse electromagnetic wave in question propagates through the plasma with a phase velocity ω/k of the order of or greater than c. Under these conditions, and subject to the requirement that $v/c \ll 1$, to a good approximation Eq. 3 is given by

$$f_1 = \frac{e}{m} \frac{\mathbf{E}_1 \cdot (\partial f/\partial \mathbf{v})}{j\omega + \nu(v)}. \tag{4}$$

From this, the RF current density $\mathbf{J}_1$ and the RF conductivity σ can be deduced with the aid of the following relations:

$$\mathbf{J}_1 = -e \int \mathbf{v} f_1\, d^3v \tag{5}$$

and

$$\mathbf{J}_1 = \sigma \mathbf{E}_1. \tag{6}$$

It is now convenient to express the velocity vector $\mathbf{v}$ in spherical coordinates (v, θ, ϕ) as illustrated in Fig. XIII-1, and to orient the electric vector $\mathbf{E}$ of the wave along the z axis (thus the propagation vector $\mathbf{k}$ of the wave lies in the x-y plane). By means of Eqs. 4-6, we then find the following expression for the conductivity σ in terms of the distribution function $f(v, \theta, \phi)$:

$$\sigma = -2\pi\epsilon_o \omega_p^2 \int_0^{\infty} \int_0^{\pi} \frac{v^3\, dv \sin\theta \cos\theta\, d\theta}{j\omega + \nu(v)} \left[\frac{\partial f}{\partial v} \cos\theta - \frac{1}{v} \frac{\partial f}{\partial \theta} \sin\theta\right]. \tag{7}$$

Here $\omega_p = \left[Ne^2/m\epsilon_o\right]^{1/2}$ is the electron plasma frequency, and the distribution f is normalized so that

$$\int f\, d^3v = 1. \tag{8}$$

We observe in passing that when f is isotropic ($\partial f/\partial\theta = 0$), the conductivity becomes

$$\sigma = -\epsilon_o\omega_p^2 \int_0^\infty \frac{4\pi}{3} v^3\, dv\, \frac{\partial f/\partial v}{j\omega + \nu(v)}, \tag{9}$$

which is a result due to Margenau[11] and to Allis.[12]

The dispersion relation for transverse electromagnetic waves can now be determined from a knowledge of σ, or from the equivalent dielectric coefficient K, through

$$k^2c^2/\omega^2 = K = 1 + \sigma/(j\omega\epsilon_o) \tag{10}$$

which, together with Eq. 7, yields the result that we sought

$$\frac{k^2c^2}{\omega^2} = 1 + 2\pi \frac{\omega_p^2}{\omega} \int_0^\infty \int_0^\pi \frac{v^3\, dv \sin\theta \cos\theta\, d\theta}{\omega - j\nu(v)} \left[\frac{\partial f}{\partial v}\cos\theta - \frac{1}{v}\frac{\partial f}{\partial\theta}\sin\theta\right]. \tag{11}$$

When $\nu(v)$ is independent of speed, Eq. 11 reduces to the familiar form

$$\frac{k^2c^2}{\omega^2} = 1 - \frac{\omega_p^2}{\omega(\omega - j\nu)}, \tag{12}$$

which exhibits no unstable solutions. Similarly, Eq. 11 exhibits no unstable solutions when f is isotropic and Maxwellian, in accord with our expectations. To study the dependence of the instability on such plasma parameters as ν, ω_p, and ω, a choice of distribution function must be made. We now address ourselves to such a special case.

Monoenergetic Electron Beam

We consider a beam of electrons of velocity v_o traveling at an angle θ_o with respect to the electric vector $\underset{\sim}{E}$ of the electromagnetic wave (see Fig. XIII-1). The appropriate distribution function for this situation is given by

$$f(v, \theta, \phi) = \left[2\pi v_o^2 \sin\theta_o\right]^{-1} \delta(v - v_o)\, \delta(\theta - \theta_o). \tag{13}$$

Substituting Eq. 13 in Eq. 11 and performing the elementary integrations, we find that

$$\frac{k^2c^2}{\omega^2} = 1 - \frac{\omega_p^2}{\omega(\omega-j\nu)}\left[1 + j\frac{\nu}{(\omega-j\nu)} R\right]. \tag{14}$$

Here the electron-ion (or electron-atom) collision frequency $\nu(v)$ is to be evaluated at $v = v_o$; and the parameter R is defined as

$$R = \left[\frac{d \ln \nu}{d \ln v}\right]_{v=v_o} \cos^2 \theta_o. \tag{15}$$

The magnitude (and the sign) of the quantity R determine the stability of the wave. When $|R| \leq 1$ the wave is stable: its amplitude either remains constant or falls exponentially with time or distance. When $|R| > 1$ a growing wave may exist. For

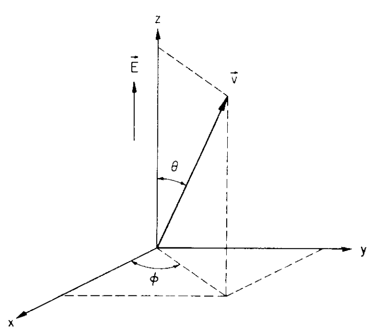

Fig. XIII-1. Coordinate system: $\underset{\sim}{E}$ is the electric field of the electromagnetic wave whose propagation vector $\underset{\sim}{k}$ lies in the x-y plane.

purposes of computation it is often convenient to approximate the interaction potential between the electron and the struck particle by a power law of the form, $\phi \propto r^{-s}$, where s is a positive number. This results[13] in a collision frequency which has a simple power-law dependence on the electron speed v

$$\nu \propto v^h \tag{16}$$

with

$$h = (s-4)/s.$$

Inserting Eq. 16 in Eq. 15, we then have

$$R = h \cos^2 \theta_o, \tag{17}$$

and the wave can be unstable only if $|h| > 1$. We also see that the instability is limited to a range of angles θ_o given by

$$\theta_o < \cos^{-1} \left(|h|^{-1/2}\right). \tag{18}$$

For Coulomb collisions, $h = -3$ and $\theta_o \approx 54.6°$. Therefore, an electromagnetic perturbation grows only if the velocity vector of the electron beam lies within a cone of cone angle equal to 110°, with the cone axis oriented parallel to the electric vector of the wave. Outside this cone the wave is damped through Coulomb collisions.

At this point one may well ask what happens when the beam electrons are incident from all possible directions θ_o, with a uniform distribution over all angles of incidence. Do the absorptions for $\theta_o > 55°$ outweigh the unstable emissions for $\theta_o < 55°$, or does the isotropic distribution of electron streams remain unstable? To answer this question we return to Eq. 11 and insert the isotropic distribution

$$f(v, \theta, \phi) = \left[4\pi v_o^2\right]^{-1} \delta(v-v_o). \tag{19}$$

This yields a dispersion relation identical to that given by Eq. 14, with R of Eq. 15 replaced by the new function,

$$R(\text{isot}) = \left(\frac{1}{3}\right)\left[\frac{d \ln \nu}{d \ln v}\right]_{v=v_o}. \tag{20}$$

It is now clear that for Coulomb collisions R(isot) = −1, and the waves are stable. This provides the basis for the statement made in the introduction that a collisional instability in an electron-ion plasma does not occur in an isotropic velocity distribution. It also confirms the findings of Twiss[8] and others.[14]

Almost without exception, analyses of collisional instabilities made by earlier workers have been confined to very tenuous plasmas in which collective phenomena are negligible, and collisions are infrequent. Here the phase velocity of the wave differs little from its free-space value of c. To make contact with these calculations, we let $\left(\omega_p^2/\omega^2\right) \ll 1$ and $(\nu/\omega) \ll 1$ in Eq. 14 to obtain

$$k^2c^2 \approx \omega^2 - j\omega_p^2(\nu/\omega)[1+R], \tag{21}$$

from which we readily deduce the absorption coefficient $\alpha \equiv -2\text{Im}k$:

$$\alpha \approx \left(\omega_p^2/\omega^2\right)(\nu/c)[1+R]. \tag{22}$$

We now adopt a more accurate expression for the electron-ion collision frequency

$$\nu(v) = 4\pi N r_o^2(c^4/v^3) \ln\left[2mv^2/h\omega\right], \tag{23}$$

where r_o is the classical electron radius, and inserting it in Eq. 22, we find that

$$\alpha = 4\pi N r_o^2 (\omega_p/\omega)^2 (c/v_o)^3 \left[\left(1 - 3\cos^2\theta_o\right) \ln\left(\frac{2mv_o^2}{h\omega}\right) + 2\cos^2\theta_o\right]. \quad (24)$$

This is precisely the result derived by Marcuse from a full quantum-mechanical calculation of stimulated emission and absorption of radiation by an electron scattered in a Coulomb potential. Since the term $\ln [2mv_o/h\omega]$ is very much greater than unity (a requirement implicit in Eq. 23), it follows that α is negative (instability) when $\cos^2\theta_o \gtrsim 1/3$, or $\theta_o \lesssim 54.6°$. This is the same instability condition that we have discussed.

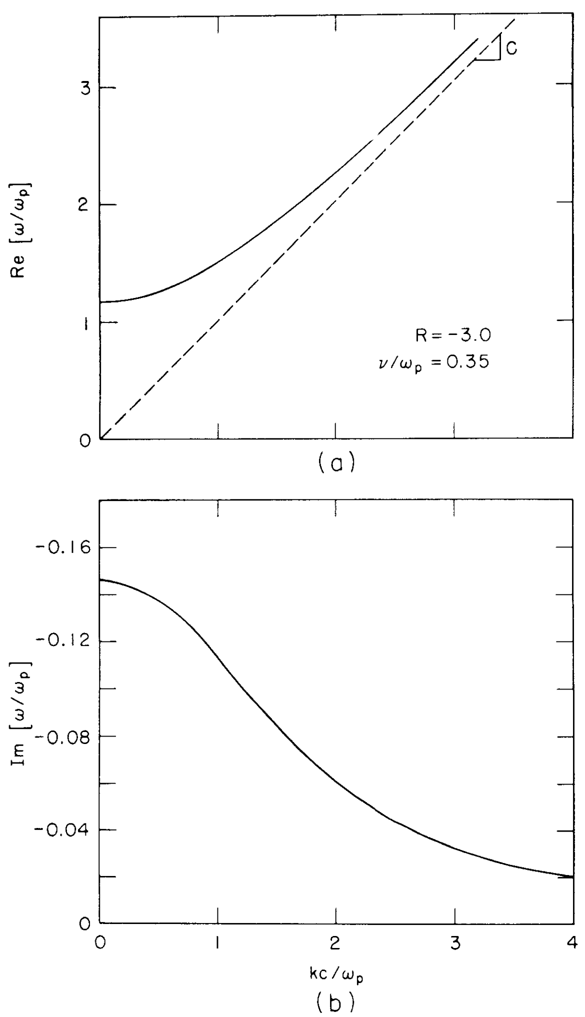

Fig. XIII-2.

Dispersion curves for real k and complex ω. Dashed line is the "light line." Note that there is no solution below the plasma frequency.

Stability Analysis

A plot of the dispersion equation (14), evaluated for real k and complex ω is illustrated in Fig. XIII-2 for one set of plasma parameters, R = −3, $\nu(v_o)/\omega_p$ = 0.35. Figure XIII-2a is typical of the propagation characteristics of a transverse electromagnetic wave traveling through an isotropic plasma not acted upon by external dc magnetic (or electric) fields: the phase velocity of the wave exceeds c and approaches infinity at low wave number. Figure XIII-2b shows that the wave is unstable (Im ω < 0) for all values of k. The growth rate of the instability is largest at k = 0, that is, at infinite wavelength. Calculations for other plasma parameters exhibit results qualitatively similar to those shown in Fig. XIII-2, provided that R < −1. For positive values of R the dispersion plots are entirely different. Since our interest is mainly with electron-ion plasmas, however, we shall not discuss cases with R > 0.

We apply the Bers-Briggs[15] test to see whether the instability in question is

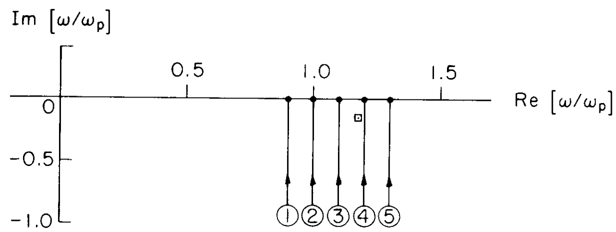

(a)

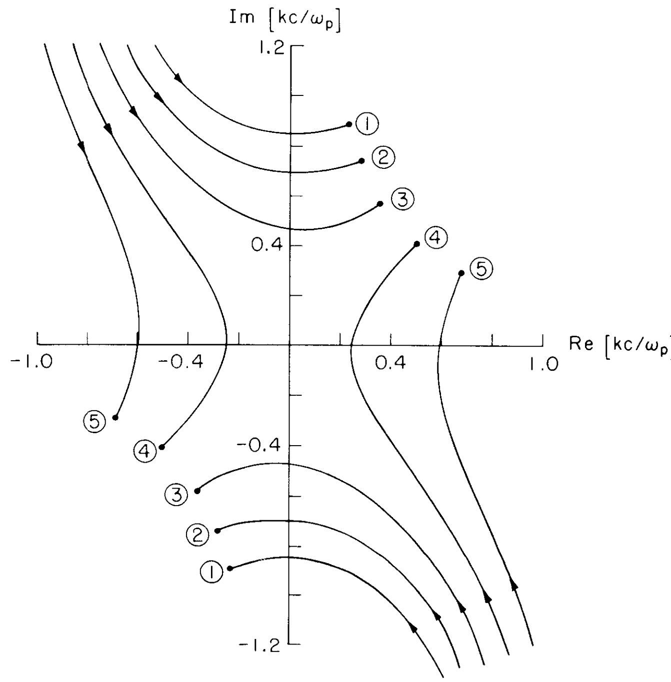

(b)

Fig. XIII-3. Stability diagram for the case R = −3, $\nu/\omega_p = 0.35$. Solid circles in (a) and (b) indicate conditions when the frequency ω is pure real. The saddle point of ω(k) [⊡] at $\omega/\omega_p \approx 1.2 - j(0.15)$ and k = 0 indicates an absolute instability.

absolute (a pulse disturbance grows in time at all points in space), or convective (the disturbance amplifies spatially). The test involves the mapping of trajectories in the complex k-plane which are generated by trajectories taken in the complex ω-plane. Specifically, we move along complex ω lines from $[\mathrm{Re}(\omega)-j(\infty)]$ to $[\mathrm{Re}(\omega)-j(0)]$ as is indicated in Fig. XIII-3a. For each such trajectory labeled (1), (2), etc. in the complex ω-plane, we map the corresponding trajectory in the complex k-plane (Fig. XIII-3b). An absolute instability occurs if two such trajectories, one from the upper half k-plane and one from the lower half k-plane, merge as ω is varied along the specified paths. In our case a merging is seen to occur at k = 0 and thus the instability is absolute. The small square in Fig. XIII-3a shows the location of the instability in the complex ω-plane.

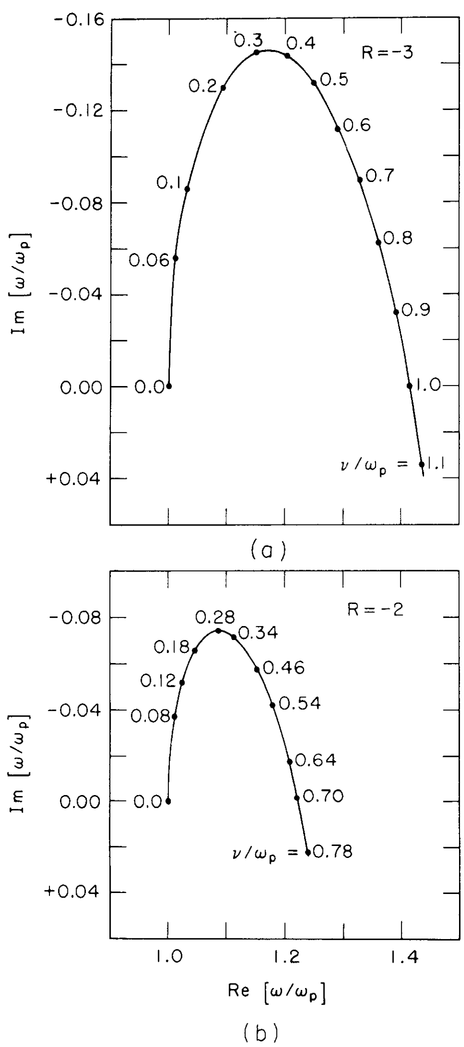

Fig. XIII-4.
Growth rate $-\mathrm{Im}\,(\omega/\omega_p)$ and frequency $\mathrm{Re}\,(\omega/\omega_p)$ of the absolute instability at k = 0, for different values of ν/ω_p and (a) R = -3, (b) R = -2.

In the context of an infinite (uniform) plasma, the absolute instability at k = 0 with ω complex is all that needs to be explored; the system will break spontaneously into oscillation at a frequency and with a growth rate appropriate to this instability. When we set k = 0 in Eq. 14, a cubic equation in ω results. One of the roots is found to be identically zero ($\mathrm{Re}\,\omega_1 = \mathrm{Im}\,\omega_1 = 0$). The two remaining roots have equal magnitudes and "reversed" signs ($\mathrm{Re}\,\omega_2 = -\mathrm{Re}\,\omega_3$, $\mathrm{Im}\,\omega_2 = \mathrm{Im}\,\omega_3$). Figure XIII-4 shows results of computations for various values of $\nu(v_o)/\omega_p$ and for two different values of the parameter R. A negative value of ω implies temporal growth of the wave. We see that the instability is confined to a narrow range of frequencies located near and above the electron plasma frequency.

When the collision frequency becomes too large the absolute instability disappears ($\mathrm{Im}\,\omega > 0$). Now, one of two possibilities arises: the plasma becomes stable or it becomes convectively unstable. The latter occurs — a fact that is illustrated in

Fig. XIII-5. Here we again map trajectories in the complex k-plane for the specific trajectories in the complex ω-plane. The crossing of the real k axis by some trajectories implies convective instabilities (those trajectories that do not cross give stable operation). Figure XIII-6 shows the corresponding dispersion curves.

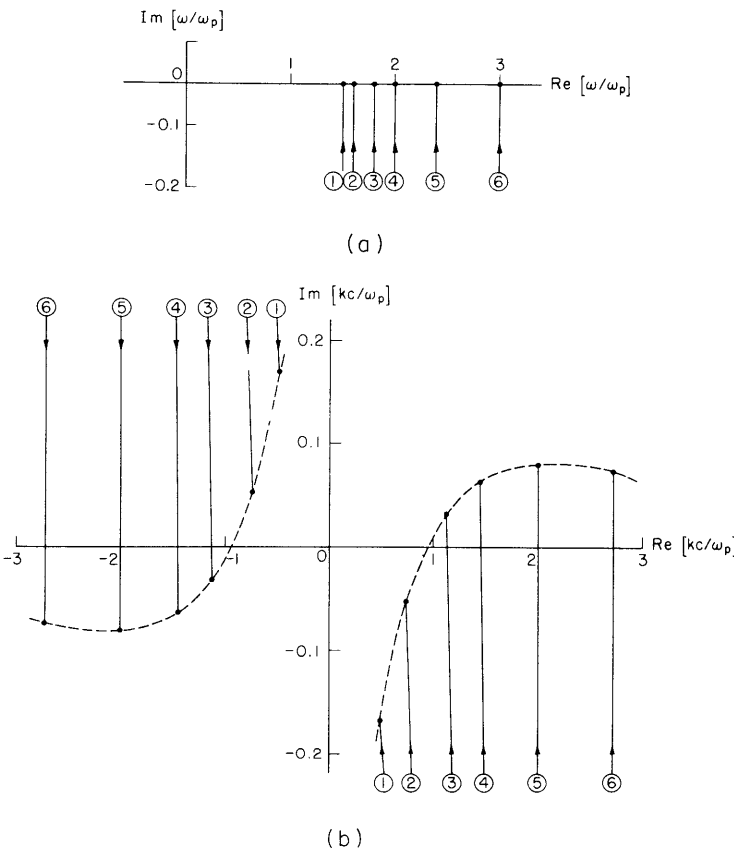

Fig. XIII-5. Stability diagram for the case R = −3, ν/ω_p = 1.2. The crossing of the real k axis in (b) indicates a convective (amplifying) wave. Trajectories that do not cross signify damped waves. Solid circles represent real ω. Dashed line joins the circles. Observe that waves traveling from left to right and from right to left amplify.

We must now stress that the plasma regime, where convective instabilities are indicated, represents a most unlikely physical situation: in the presence of the required high collision rates, the electron beam will not maintain its identity for a sufficiently long time. Indeed, we suspect that the beam will survive only when $\nu(v_o)/\omega_p \ll 1$. Under these conditions, the dispersion equation (14) takes on the simpler form

$$\frac{k^2c^2}{\omega^2} \approx 1 - \frac{\omega_p^2}{\omega^2} - j\,\frac{\omega_p^2}{\omega^2}\,\frac{\nu}{\omega}\,[1+R]. \tag{25}$$

From this equation we readily find that the absolute instability located at $k = 0$, $\mathrm{Re}\,\omega \approx \omega_p$, has a growth rate given by

$$\mathrm{Im}\,\omega = \frac{1}{2}\,\nu(v_o)[1+R]; \qquad [\nu/\omega_p \ll 1], \tag{26}$$

which we can write in a more useful form as

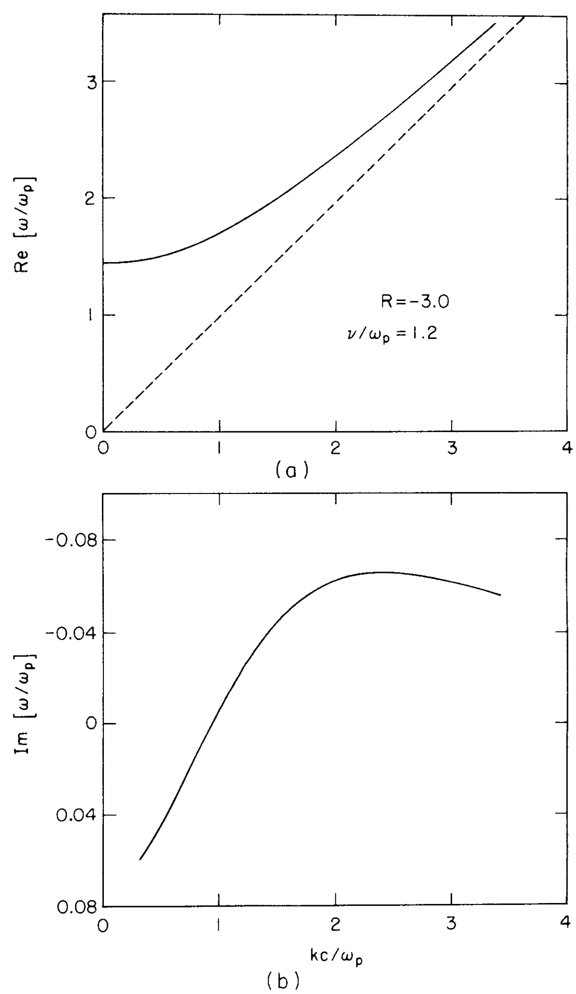

Fig. XIII-6. Dispersion curves for real k and complex ω for the same plasma parameters as those considered in Fig. XIII-5. Observe that there is a threshold value of kc/ω_p below which the wave damps.

$$\mathrm{Im}\left(\frac{\omega}{\omega_p}\right) = \frac{1}{2}\left(\frac{\nu}{\omega_p}\right)[1+R]. \tag{27}$$

For an electron-ion plasma the ratio ν/ω_p appearing on the right-hand side of Eq. 27 has a particularly simple form. Using the value of ν given by Eq. 23, we find that

$$(\nu/\omega_p) \approx [3N_D]^{-1} \ln \Lambda, \tag{28}$$

where $N_D = (4\pi/3)L_D^3N$ is the number of particles in the Debye sphere, L_D is the Debye length, and $\Lambda \approx [2mv_o^2/h\omega]$. Most plasmas of interest have a value of N_D between, say, 10 and 10^4. The parameter $\ln \Lambda$ is of order 10. Thus, the expected growth rates are $\mathrm{Im}(\omega) \approx z\omega_p$, where the numerical coefficient z ranges between 10^{-1} and 10^{-4}.

Conclusions

We have shown that a collisional, Bremsstrahlung instability can be stimulated in an electron-ion plasma, provided that the distribution of electron velocities is sufficiently anisotropic. For reasons of simplicity, we have considered only the idealized model of a monoenergetic electron stream. More realistic distributions, for example, a drifted Maxwellian, should be examined.

A stability analysis has shown that for $\nu/\omega \ll 1$, the instability is absolute and occurs only over a very narrow frequency band near and above the electron plasma frequency. Hence in the context of an infinite (homogeneous) plasma the system breaks out spontaneously into oscillation and behaves somewhat like a very narrow-band oscillator. Therefore, the use of this instability as a wideband amplifier, as implied by Ensley[7] and Marcuse,[9] is at present unfounded. Of course, difficulties of interpretation arise in regard to the behavior of a physical system which of necessity is of finite size. This difficulty is particularly great in our case when we find that the absolute instability is associated with an infinite wavelength (k = 0). An analysis of this instability for a bounded system has not yet been carried out.

We wish to thank J. Woo, a student in the Department of Physics, M.I.T., for his assistance with computer programming.

G. Bekefi

References

1. G. Bekefi, J. L. Hirshfield, and S. C. Brown, Phys. Fluids 4, 173 (1961); J. A. Howell, Report SUIPR No. 364, Institute for Plasma Research, Stanford University, May 1970.

2. G. Bekefi, Radiation Processes in Plasmas (John Wiley and Sons, Inc., New York, 1966), p. 286.

3. Ibid., p. 306-310.

4. S. Ohara, J. Phys. Soc. Japan 18, 852 (1963); S. J. Tanaka, H. Honzawa, H. Ikegami, and K. Takayama, Report No. IPPJ-32 (1964), Institute of Plasma Physics, Nagoya University; S. Tanaka and K. Mitani, J. Phys. Soc. Japan 19, 1376 (1964); K. Mitani, S. Tanaka, and Y. Terumichi, VIIth International Conference on Phenomena in Ionized Gases, Belgrade 1965 (Gradevinska Knjiga, Beograd, Yugoslavia, 1966); J. M. Wachtel and J. L. Hirshfield, Phys. Rev. Letters 19, 293 (1967); C. Oddou, Thesis, Faculté de Sciences de L'Université de Paris, 1971.

5. P. F. Browne, Astrophys. J. 134, 963 (1961); 136, 442 (1962). (The conclusions reached in these papers are wrong as was later demonstrated by the last two works of ref. 8.)

6. T. P. Hughes and M. B. Nicholson-Florence, J. Phys. A 1, 558 (1968); M. B. Nicholson-Florence, J. Phys. A 4, 574 (1971).

7. D. L. Ensley, Harvest Queen Mill and Elevator Company, Dallas, Texas (unpublished report, January 5, 1971).

8. R. Q. Twiss, Australian J. Phys. 11, 564 (1958); Astrophys. J. 136, 438 (1962); P. Mallozzi and H. Margenau, Astrophys. J. 137, 851 (1963).

9. D. Marcuse, Bell System Tech. J. 41, 1557 (1962); 42, 415 (1963).

10. F. V. Bunkin and M. V. Fedorov, Soviet Phys. – JETP 22, 844 (1966) [J. Exptl. Theoret. Phys. USSR 49, 1215 (1965)].

11. H. Margenau, Phys. Rev. 69, 508 (1946); 109, 6 (1958).

12. W. P. Allis, "Motions of Ions and Electrons," in S. Flügge (Ed.), Handbuch der Physik, Vol. 21 (Springer Verlag, Berlin, 1956), pp. 383-444.

13. H. M. Mott-Smith, Phys. Fluids 3, 721 (1960).

14. S. C. Brown and G. Bekefi, "Radio-Frequency Emission from Plasmas Not in Thermodynamic Equilibrium," Nuclear Fusion, 1962 Supp., Part 3, pp. 1089-1099.

15. A. Bers and R. J. Briggs, Quarterly Progress Report No. 71, Research Laboratory of Electronics, M.I.T., October 15, 1963, pp. 122-130; R. J. Briggs, Electron-Stream Interaction with Plasmas (The M.I.T. Press, Cambridge, Mass., 1964), Chap. 2.

2. STEADY-STATE LINEAR MULTIPOLE (SLIM-1)

The steady-state linear quadrupole has been in operation since August 1971.[1] During this period the mechanical operation of the device has been tested and preliminary studies of the equilibrium plasma configuration have been carried out. The maximum current attainable in each of the conducting bars is 75 kA, limited by the allowable output voltage of the motor-generator set. At this current level the quadrupole magnet dissipates 1.65 MW. With the normal conductor separation of 32.7 cm, this current gives a 2600-G peak magnetic field strength on the separatrix. At this field the ion Larmor radius is approximately 1 mm (He^+; $T \sim 0.25$ eV). Because of currents in external conductors, the magnetic axis is displaced by 1.5 cm out of the plane of the quadrupole bars. The vacuum system has worked well and is regularly pumped to a base pressure of 3×10^{-7} Torr in 24 h without baking.

Attempts to produce a plasma by using a slotted cylinder concentric with the magnetic axis to couple RF power into the system did not work well. The plasma was very nonuniform and was localized in the neighborhood of the magnetic field lines passing through the cylinder slots. At present the plasma is produced with the use of the vacuum chamber as a high-mode number cavity. Approximately 150 W of cw power at 4.5 GHz are coupled into the cavity through an iris. Under all conditions the reflected power is less than 1%. An RF source providing up to 500 W at X-band has been obtained and will be installed soon. This will allow operation at lower densities (longer mean-free paths) than at present. The discharge is initiated by electron-cyclotron resonance and power is absorbed by the plasma at both the electron-cyclotron and upper hybrid frequencies over a large part of the plasma volume. Approximate power balance calculations indicate that at least 20% of the RF power is being absorbed by the plasma.

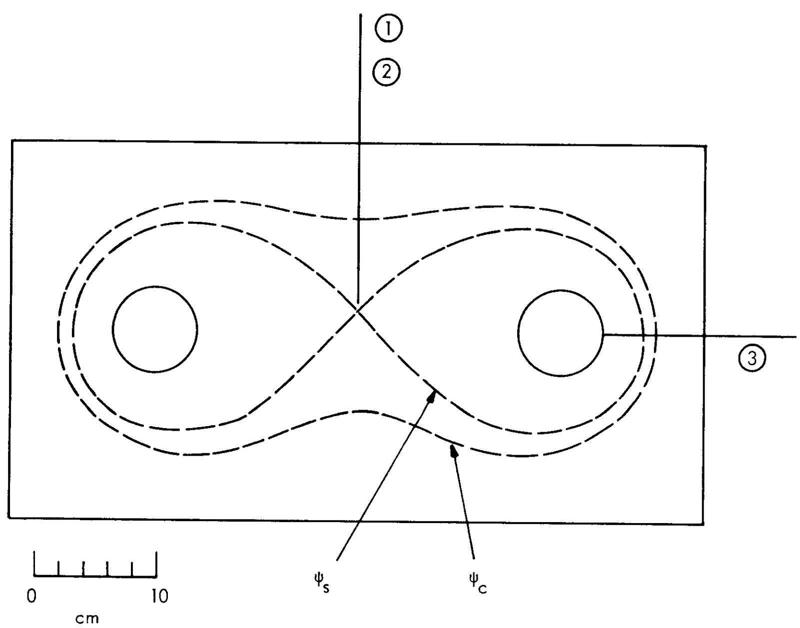

Fig. XIII-7. Cross section of the device showing the locations of the separatrix ψ_s and critical field line ψ_c, as well as the paths of the three movable probes.

A "radial" scan (Fig. XIII-7) of the ion saturation current collected by a Langmuir probe shows that the plasma density is bell-shaped, centered at, or just inside of, the separatrix. It can be fairly well fitted by a Gaussian function (Fig. XIII-8). The electron temperature is uniform (±20%) across the radius and varies between 10 eV and 20 eV,

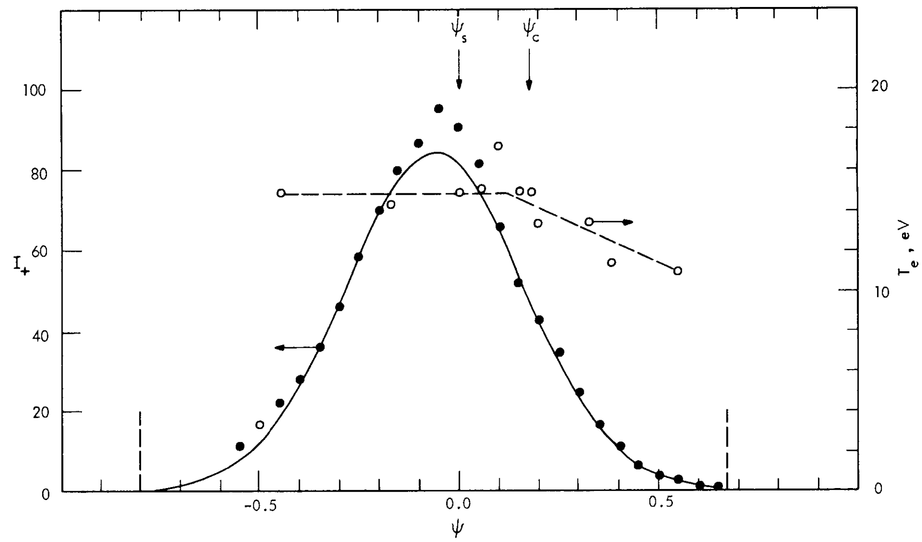

Fig. XIII-8. Scan of ion saturation current and electron temperature measured by Probe 3. Vertical dashed lines show positions of conducting bar and vacuum chamber wall.

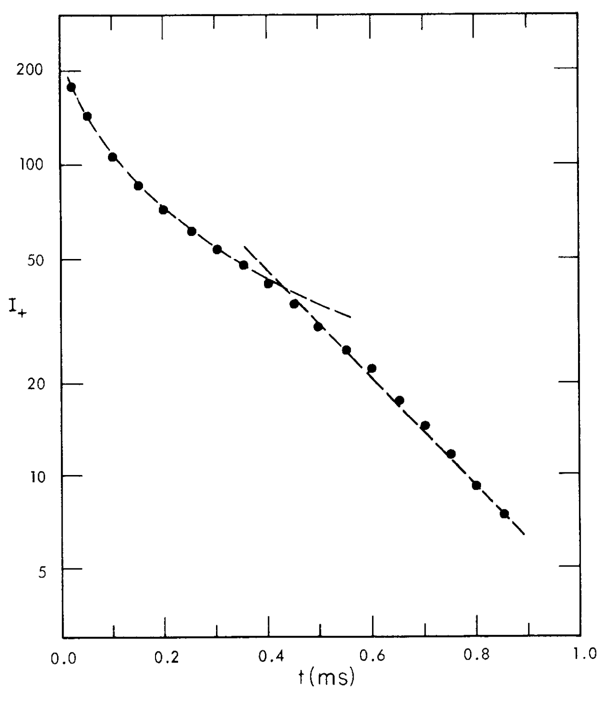

Fig. XIII-9. Decay of ion saturation current with time. RF power off at t = 0. Points for $t < 0.4$ ms fitted by $(1+\alpha t)^{-1}$ and for $t > 0.4$ ms by $\exp -\beta t$. ($\alpha = 10.9 \times 10^3\ s^{-1}$; $\beta = 3.6 \times 10^3\ s^{-1}$.)

depending upon the external parameters – magnetic field, neutral pressure, and RF power. The maximum density obtained is $\sim 1.5 \times 10^{11}$ cm^{-3}. The plasma containment time is in agreement with the time required for the plasma to flow to the ends of the system because of grad B drifts. This time is measured by looking at the density decay when the RF power is turned off (Fig. XIII-9). There appear to be two regimes of decay. Initially the plasma density is proportional to 1/t, and then goes over to an exponential decay. The characteristic time for containment is approximately 0.5 ms.

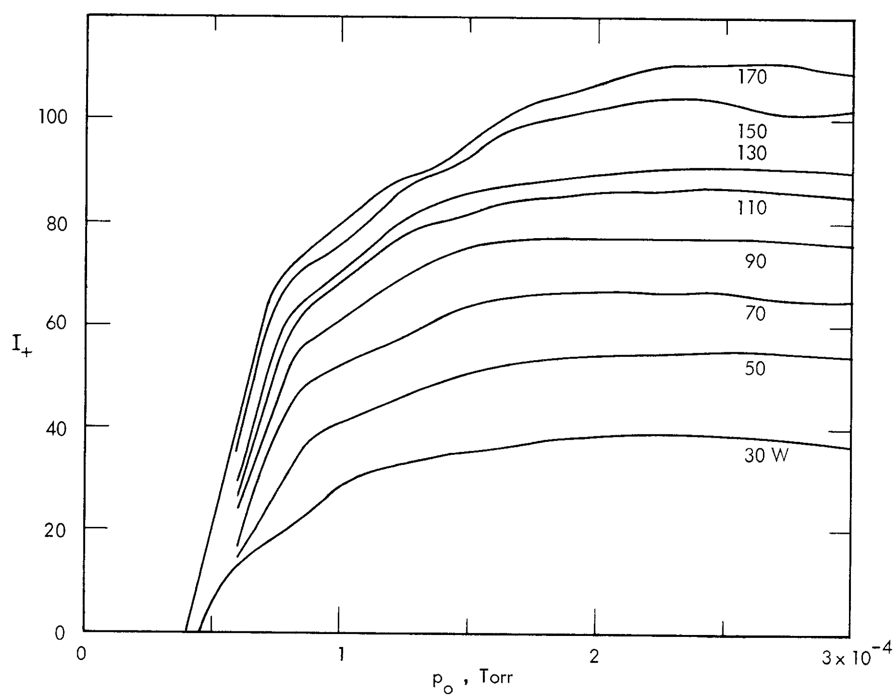

Fig. XIII-10. Ion saturation current vs neutral gas filling pressure with RF power as a parameter.

The plasma density variation with RF power and with neutral filling pressure has been investigated (Fig. XIII-10). The variation of density with power is $n \propto P^a$, with $1 > a > 1/2$. As a function of filling pressure, the discharge cannot be sustained below $\sim 4 \times 10^{-5}$ Torr (in helium). Between 4×10^{-5} and 1×10^{-4} Torr the density increases rapidly, approaching a maximum of ~6% ionization. Above this pressure the density stays approximately constant. At maximum available RF power the density is such that $(\omega_p/\omega)^2 \approx 1/2$. The dependence of density on neutral pressure can be explained in terms of competition between several different loss mechanisms. If the continuity equation is written in the form

$$\frac{\partial n}{\partial t} = \nu_i n - \alpha n^2 - \beta n,$$

where the second term may represent classical diffusion and the third may indicate particle drifts to the walls, the observed behavior is qualitatively explained. In equilibrium, breakdown occurs at a neutral pressure given by $\nu_i(n_o) = \beta$, and the plasma density then increases rapidly with increasing n_o: $\partial n/\partial n_o = \nu_i/n_o\alpha$. If the RF power is shut off, the density decay is given by

$$n = n(0) \frac{e^{-\beta t}}{1 + \frac{\alpha n(0)}{\beta} (1-e^{-\beta t})}$$

which at first shows an $n \propto 1/t$ dependence, and then goes over to an exponential decay. As noted, the magnitude of the containment time is in agreement with the grad B drift time $(1/\beta)$, but more accurate identification of the coefficients α and β with definite physical phenomena must await further measurements of their dependences on plasma temperature and magnetic field.

P. A. Politzer

References

1. P. A. Politzer, Quarterly Progress Report No. 96, Research Laboratory of Electronics, M.I.T., January 15, 1970, pp. 85-87.

XIII. PLASMAS AND CONTROLLED NUCLEAR FUSION*

B. Diffusion and Turbulence

Academic Research Staff

Prof. T. H. Dupree
Prof. L. M. Lidsky

Graduate Students

K. R. S. Chen
D. L. Ehst
P. M. Margosian
G. K. McCormick
A. Pant
N. R. Southoff
A. E. Wright

RESEARCH OBJECTIVES AND SUMMARY OF RESEARCH

1. Toroidal Electron Trap

Our original experiment for measuring the lifetime of electrons circulating in a toroidal magnetic trap has been completed. The technology needed to inject electrons and to measure their lifetimes has been perfected. A sweeping system to allow measurement of the angular distribution of the circulating electrons has been built and is being tested. This apparatus will be used for the study of waves propagating on electron beams and as a test bed for some experiments to be done on Alcator. To this end, we have designed an electrode structure to give us a phase-stabilized beam. This will be used for the accurate mapping of flux surfaces.

P. M. Margosian, L. M. Lidsky

2. Incoherent Scattering – Anisotropic Velocity Distribution

We are using incoherent scattering techniques to measure the distribution of plasma electron velocities in the directions parallel and perpendicular to the confining magnetic field. Experiments show that the electron temperature in the HCD plasma is isotropic in normal operation. The experiment strives for high accuracy, and is highly automated to serve as a test of the forthcoming Alcator Thomson scattering experiment.

G. K. McCormick, L. M. Lidsky

3. Coherent Scattering from Steady-State Plasmas

We are attempting to observe coherent scattering of 10.6 μ radiation from the moderate density steady-state plasma produced by the hollow-cathode discharge source. Our goal is the comparison of the experimentally measured and theoretically predicted scattered spectra in order to determine the spectrum of plasma density fluctuations, that is, to measure plasma turbulence. We are using a 100-W N_2-CO_2He laser as a radiation source and cryogenic Ge detectors.

Measurements of signal-noise ratios for the separate parts of this system have been completed. It appears that final S/N ratios of 6 are achievable. We hope to observe the detailed structure of the plasma-frequency satellites.

K. R. S. Chen, L. M. Lidsky

*This work is supported by the U.S. Atomic Energy Commission (Contract AT(11-1)-3070).

4. Superconducting Magnet Design Studies

It is clear that high-field steady-state plasma confinement experiments will require the use of superconducting coils. We are studying the applicability of superconductor technology to various toroidal plasma systems. We are studying, in particular, the design problems of a 100-kG neutral ion-injected Tokamak experiment and of a uni-conductor high-shear stellarator. In order to gain direct experience working with modern superconducting materials, we have constructed a single low-field element of a possible linear quadrupole pair.

A. E. Wright, L. M. Lidsky

XIII. PLASMAS AND CONTROLLED NUCLEAR FUSION*

C. Plasma Diagnostics

Academic and Research Staff

Prof. G. Bekefi
Prof. E. V. George
Dr. P. A. Politzer

Graduate Students

R. J. Hawryluk

RESEARCH OBJECTIVES

The major goals of this program are to perfect known methods of measuring plasma properties and to devise new techniques. Our present interest concerns the use of optical spectroscopy in the diagnosis of dense, turbulent plasmas. The turbulent electric fields acting on excited atoms can cause a splitting of energy levels with the result that new spectral lines may become evident. These can then be used to determine the intensity and spectral distribution of the fluctuating fields. In the studies we use two types of plasma sources, plasmas produced by focusing intense laser radiation on gas or solid targets, and plasmas produced in a recently constructed coaxial plasma gun.

G. Bekefi

*This work was supported by the U. S. Atomic Energy Commission (Contract AT(11-1)-3070).

XIII. PLASMAS AND CONTROLLED NUCLEAR FUSION*

D. Fusion-Related Studies

Academic Research Staff

Prof. L. M. Lidsky
Prof. R. A. Blanken
Prof. R. J. Briggs

Graduate Students

G. W. Brown
R. L. McCrory

RESEARCH OBJECTIVES

1. Fusion Feasibility

We will continue our work on the analysis of fusion power systems with particular emphasis given to the possibilities inherent in fission-fusion symbiosis. The combination of a marginal D-T fusion reactor with an MSCR fission reactor operating on the thorium cycle will be analyzed in more detail. Another system to be studied during the next year is the D-D cycle mirror reactor with direct conversion. It appears that efficient use of the neutrons generated in the complete D-D cycle may suffice to make this concept economically viable also.

L. M. Lidsky

2. Economics of Reactor Concepts

All known fusion reactor concepts contain some difficult physical questions that are often overlooked in the simple economic analyses done thus far. We plan to analyze several of the more important of these to see their effect on fusion reactor economics. For example, there is considerable experimental and theoretical evidence that the maximum allowable β in toroidal systems will be a strong function of the aspect ratio. Studies of the economics of toroidal reactors are being undertaken using realistic assumptions for the functional dependences of β on the aspect ratio. For another example, the crucial problems of synchrotron radiation have been handled very approximately in previous studies. A re-examination of the economics of mirror reactors using more realistic models for radiation reabsorption is under way.

R. A. Blanken

*This work is supported by the U.S. Atomic Energy Commission (Contract AT(11-1)-3070).

E. Feedback Stabilization

Academic Research Staff

Prof. R. R. Parker
Prof. L. D. Smullin
Prof. K. I. Thomassen

Graduate Students

R. S. Lowder
A. R. Millner

RESEARCH OBJECTIVES

The objectives of this research are to use feedback control techniques for the diagnostic study and suppression of instabilities in plasmas. Under investigation are ways to couple the feedback system to the plasma, the applicability of this method to fusion devices, and the study of continuum feedback methods in general.

Present studies include investigations of the drift instability in a moderately energetic plasma (10^{12} density, 15 eV temperature) and ways to couple to it, MHD instabilities in a Tokamak and coupling schemes for their suppression, and adaptation of the methods of modern control theory to the general problem of continuum feedback control.

R. R. Parker, K. I. Thomassen

1. PRELIMINARY INVESTIGATION OF PLASMA INJECTION TECHNIQUES

Injection of energetic particles into the toroidal Alcator has been proposed as a possible means of heating the confined plasma. Because of the intense magnetic induction inside Alcator, great difficulties might be anticipated in any attempt to inject unneutralized particles as, for example, ion beams. Primary consideration has therefore been given to various types of plasma and neutralized ion guns as sources for particle injection. It has been demonstrated by Bostick[1] and others[2,3] that neutralized beams, when they are dense enough ($\geq 10^{11}$ cm^{-3}) will penetrate intense transverse B-fields while maintaining directed velocities of order 10^6 cm/s. The polarization E-field, resulting from the initial $q(v \times B)$ force which tends to separate ions and electrons in the beam, is sufficient to allow the beam to drift across the magnetic field ($E \times B$ drift). Thus, the type of gun that we seek must be capable of producing a high-velocity (high-energy if it is to be used for heating a plasma), high-density neutral beam.

A type of plasma gun which may have the desired characteristics is the Marshall

*This work is supported by the U.S. Atomic Energy Commission (Contract AT(11-1)-3070.

coaxial hydromagnetic gun.[2] Plasma velocity equal to, or greater than, 10^7 cm/s and density $\sim 10^{12}$ cm^{-3} has been observed. Another attractive feature is the low percentage of contaminants appearing in the plasma even at high currents (10^5 A). We would like to know the particular gun parameters involved in determining the velocity and density of the emitted plasma.

By treating the moving (velocity V_s) current sheath between the coaxial electrodes as a magnetic piston from which ionized particles ahead of it gain momentum at a rate $dp/dt = 2\rho_M \pi \left(r_o^2 - r_i^2\right) V_s^2$, and equating this with the electromechanical force resulting from the changing inductance ($f_m = \frac{1}{2} \mathscr{L} i^2$, where $\mathscr{L} = \partial L/\partial Z$, and Z is the axial direction) it has been found[4] that after one current cycle, a maximum of 75% of the energy stored initially in the capacitor banks (energy that is used to initiate breakdown and drive the sheath) is converted into plasma energy. Usually, this figure is closer to 40% because of unavoidable stray inductances in the feed system. Furthermore, the analysis shows that a fraction of a current cycle will usually impart less than the same fraction of this maximum energy. Therefore, we must design our gun so that it is at least long enough for the plasma to be accelerated for a minimum of one current cycle, approximately 10 μs, which gives a typical length of 50 cm.

These comments reflect the direction of our intended research. We would like to understand better the resulting evolution of the plasma once it leaves the gun. The features of the gun that will ultimately limit its desirable characteristics are still obscure, but will be studied. Also, we would like to investigate further the nature of the breakdown in the gun to determine the finite mass of the current sheath, which because of "snowplowing" effects may be a limiting factor for the ultimate attainable velocities. All of these features must be understood before a suitable injection device for Alcator can be proposed.

L. D. Smullin, S. P. Hirshman

References

1. W. H. Bostick, "Experimental Study of Ionized Matter Projected across a Magnetic Field," Phys. Rev. 104 (1956).

2. J. Marshall, "Hydromagnetic Plasma Gun," in S. W. Kash (Ed.), Plasma Acceleration (Stanford University Press, Stanford, Calif., 1960).

3. R. G. Meyerand, Jr., "Interaction of Plasma Beam with Magnetic Field," Sc.D. Thesis, Department of Nuclear Engineering, M.I.T., June 1959 (unpublished).

4. S. W. Kash, "Efficiency Considerations in Electrical Propulsion," in S. W. Kash (Ed.), Plasma Acceleration (Stanford University Press, Stanford, Calif., 1960).

2. ENERGY CONSIDERATIONS RELEVANT TO KINK MODES AND TO THEIR FEEDBACK CONTROL

In previous Quarterly Progress Reports[1] stability criteria for kink modes that included feedback effects were presented. Standard MHD techniques and a new model derived in terms of particle drifts were employed. We now report another approach in which we attempt to compute changes in kinetic and magnetic energy. We invoke conservation of energy to obtain a stability criterion and to find externally imposed feedback fields for feedback stabilization. We obtain expressions for the energy of the kink modes and reveal difficulty with this method. Finally, we consider kink modes in a rotating plasma. We find that action (wave energy over frequency) is conserved and that propagating waves can be negative-energy modes; in this case resistive walls cause wave growth. The resistive wall damping and growth rates are computed.

The energy viewpoint presented here allows us to identify the sources of instability and illustrates the role of feedback as a stabilizing energy source. We take the difference between the energy in a control volume that corresponds to the perturbed plasma volume at time t and the energy in the unperturbed volume, and use Poynting's vector to keep track of the energy flow in and out of this volume. This approach, as opposed to using Bernstein's energy principle[2] directly, is a convenient way to include an external energy source such as our feedback coils, and to compute the energy required by the feedback system.

A difficulty with this approach is in accounting for second-order quantities, whose product with zero-order quantities may or may not make a negligible contribution to the change in energy. Interestingly, if they are dropped and we keep only zero- and first-order fields, we recover the terms of Bernstein's energy principle. Thus far, we have not estimated the size of the products of zero- and second-order terms, and hence we cannot identify all energy sources individually. Instead we have the "artificial energy" of the usual energy principle. Nevertheless, we can find a stability criterion with feedback and give order-of-magnitude energy requirements for feedback systems.

Statement of the Problem

The plasma, with radius a, is cylindrical, and carries both distributed and sheet currents. The distributed current has a uniform current density, j_0, out to r = a, and is a fraction, f, of the total current I_z. A sheet current at r = a carries (1-f) of the total current. Then the azimuthal field B_θ is

$$B_\theta = \begin{cases} f\,\frac{r}{a}\,B_a & r < a \\ \frac{a}{r}\,B_a & r > a \end{cases} \qquad (1)$$

where $B_a = \frac{\mu_0 I_z}{2\pi a}$. Thus, f = 1 corresponds to a flat current profile, f = 0 corresponds to a sheet pinch, $f \lesssim 1$ corresponds to a flat current distribution with a small skin current, and f > 1, in some sense, corresponds to a decreasing current distribution.

Feedback System

The kink modes and the feedback system are shown in Fig. XIII-11. The kink modes are helical perturbations about the plasma column. The helical feedback coils have the

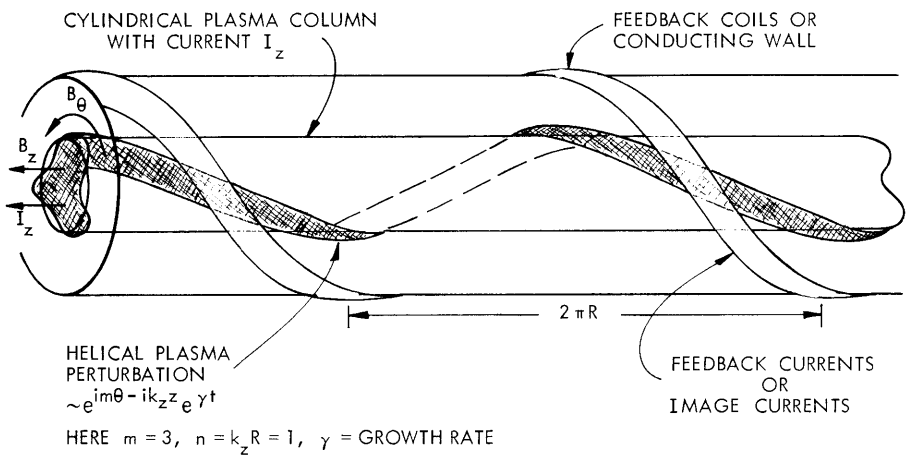

Fig. XIII-11. Kink modes and feedback system.

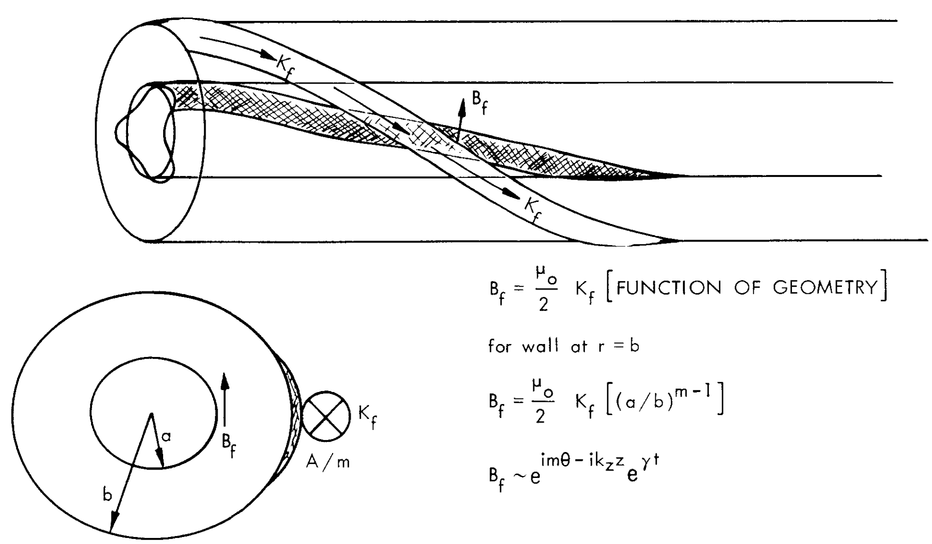

Fig. XIII-12. Kink modes and feedback field. B_f is the externally produced vacuum field at r = a.

same pitch as the perturbation. These coils carry feedback currents that are spatially and temporally like the image currents on a conducting wall, except that their amplitude and phase relative to the perturbation are now kept arbitrary.

We give all of our results (Fig. XIII-12) in terms of the feedback field B_f, the azimuthal component at $r = a$ of the vacuum field produced by the feedback current K_f. In this way, details of the geometry of the external feedback coils and walls do not enter into the equations. From the requirements on B_f, we can compute current or gain requirements for any particular external geometry and sensing arrangement.

Energy Changes

Consider the control volume illustrated in Fig. XIII-13, with its boundary at $r = a + \xi_{a0}(t'=t)\exp(im\theta - ik_z z)$. Here, $\xi_{a0}(t')$ is the magnitude of the radial component of the displacement vector $\underline{\xi}$ at $r = a$ and at time t' and has the time dependence $e^{\gamma t'}$. At time $t' = t$, the boundary of the control volume coincides with the perturbed plasma-vacuum interface.

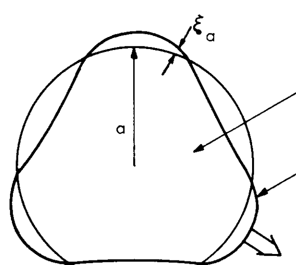

Fig. XIII-13. Control volume and energy outflow.
$W_{\Delta B^2}$ = increase in magnetic energy within volume $+\int_{-\infty}^{t} dt' \int_{surface} dS \left(\frac{1}{\mu_0} \tilde{\underline{E}} \times \underline{B}\right)$.
$W_{\Delta KE}$ = increase in kinetic energy within volume for growing waves, $W_{\Delta B^2} + W_{\Delta KE} = 0$.
Note: Only $\int_{-\infty}^{t} dt' \int_{surface} dS \left(\frac{1}{\mu_0} \tilde{\underline{E}} \times \tilde{\underline{B}}\right)$ contains B_f.

We integrate the energy conservation equation over this volume and over time t' from $-\infty$ to t. This gives

$$\iiint \Delta W_{total}\, dV + \int_{-\infty}^{t} dt' \iint \underline{F} \cdot \underline{dS} = 0, \qquad (2)$$

where ΔW_{total} is the change in the total energy density in fields and particles between

$t' = -\infty$ and $t' = t$, and $\underline{F}$ is the Poynting flow of electromagnetic energy plus the flow of particle energy.

This expression can be simplified in several ways. First, we neglect the stored electrostatic energy and hence rule out interchange flutes. Second, we assume a divergence-free surface perturbation so that there is no change in the stored thermal energy. Finally, the flow of energy carried across the bounding surface averages to zero because there is as much flux leaving the surface at the bulges as there is entering at the depressions. With these simplification Eq. 2 becomes

$$\Delta \iint \frac{B^2}{2\mu_0}\, dV + \Delta \iint \frac{1}{2}\rho v^2\, dV + \int_{-\infty}^{t} dt' \int \frac{\underline{E} \times \underline{B}}{\mu_0} \cdot \underline{dS} = 0,$$

where B is the total magnetic field, ρ is the mass density, E the electric field, and v the fluid velocity.

Expanding the fields and retaining only terms to second order in the fields gives

$$\int \frac{B_1^2}{2\mu_0}\, dV + \int \frac{\underline{B_0} \cdot \underline{B_1}}{\mu_0}\, dV + \int \frac{\underline{B_0} \cdot \underline{B_2}}{\mu_0}\, dV + \int \frac{1}{2}\rho\gamma^2\xi^2\, dV$$

$$= -\int_{-\infty}^{t} dt' \int \left(\frac{\underline{E_1} \times \underline{B_0}}{\mu_0} + \frac{\underline{E_1} \times \underline{B_1}}{\mu_0} + \frac{\underline{E_2} \times \underline{B_0}}{\mu_0} \right) \cdot \underline{dS} \qquad (3)$$

where ξ is the magnitude of the displacement vector $\underline{\xi}$, and the time dependence $e^{\gamma t'}$ is used. The difficulty with this method becomes apparent here, since second-order field quantities are required. By dropping terms with second-order fields, we recover all terms of the Bernstein energy conservation equation, as we will show. For the moment, we compute the five remaining terms.

Using the displacements[3] appropriate to modes having $k_z a \ll 1$,

$$\xi_r = (r/a)^{m-1}\, \xi_a = -i\xi_\theta$$

$$\xi_z \approx 0,$$

we find that W_{KE}, the stored kinetic energy per unit length in the plasma motion from $E \times B$ drifting, is

$$W_{KE} = \int_0^a dr \int_0^{2\pi} r\, d\theta\, \frac{1}{2}\rho\gamma^2\xi^2 = \int_0^a 2\pi r\left(\frac{1}{2}\rho\gamma^2\xi_{a0}^2\right)\left(\frac{r}{a}\right)^{2m-2}$$

$$= \frac{\pi\xi_{a0}^2}{m}\left(\frac{1}{2}\rho\gamma^2 a^2\right). \tag{4}$$

Next we compute W_{B11}, the change in magnetic energy arising from the square of the first-order magnetic field, a positive quantity. The perturbed field $\underline{B_1}$ is

$$B_{1r} = ik_{\|}B\xi_r$$

$$B_{1\theta} = ik_{\|}B\xi_\theta - r\frac{\partial}{\partial r}(B_\theta/r)\xi_r - B_\theta\nabla\cdot\underline{\xi}$$

$$B_{1z} = ik_{\|}B\xi_z - \left(\frac{\partial}{\partial r}B_z\right)\xi_r - B_z\nabla\cdot\underline{\xi},$$

where $k_{\|}$ is

$$k_{\|} = \left(\frac{m}{r}B_\theta - k_zB_z\right)/B$$

and B is $|B_0|$. Letting $k_z = n/R$ and $aB_z/RB_a = q_a$ and noting that inside the plasma $B_\theta = fB_a(r/a)$, we have

$$k_{\|} = (fm-nq_a)(B_a/aB).$$

For this current distribution $k_{\|}B$ is independent of radius, and $|\underline{B_1}| = k_{\|}B\xi_{a0}(r/a)^{m-1}$ and W_{B11} is

$$WB_{11} = \int_0^a dr\int_0^{2\pi} r\, d\theta\, \frac{1}{2\mu_0}\left[(fm-nq_a)^2\left(\frac{\xi_{a0}^2B_a^2}{a^2 2\mu_0}\right)\right]$$

$$= \frac{\pi\xi_{a0}^2}{m}\left[(fm-nq_a)^2\frac{B_a^2}{2\mu_0}\right]. \tag{5}$$

Now, to compute $W_{B01} = \int \underline{B_0}\cdot\underline{B_1}/\mu_0$, we note that the integration in azimuth is alternatively positive and negative except in the small region within ξ_a of the boundary. Within this region, the magnetic field $\underline{\delta B}$ attributable to the current strip $\mu_0 j_0\xi_a$ reverses direction in that region as the current strip is moved out to the perturbed boundary. Thus W_{B01} is quadratic in ξ_{a0}, and we have

$$W_{B01} = \int 2\left(\frac{\underline{\delta B}\cdot\underline{B}}{\mu_0}\right)dA$$

$$= m\int_0^{2\pi/2m}\left[ad\theta\xi_{a0}\cos m\theta\right]\frac{2}{\mu_0}\,\underline{\delta B}\cdot\underline{B_0},$$

where

$$\underline{\delta B}\cdot\underline{B_0} = -\delta B\left(\frac{k_{\|}}{k}\right)B$$

and

$$\delta B = \frac{\mu_0 j_0\xi_{a0}\cos m\theta}{2} = fB_a(\xi_{a0}/a)\cos m\theta$$

with $k_{\|}B$ as given above, and $k \approx m/a$. Thus we have

$$W_{B01} = -\frac{\pi\xi_{a0}^2}{m}\left(\frac{fB_a^2}{2\mu_0}\right)2(fm-nq_a). \tag{6}$$

We next define W_{E11} as the time integral of the Poynting flow $\underline{E_1}\times\underline{B_{1v}}$ across the boundary. Here, $\underline{B_{1v}} = \nabla\psi$ is the perturbed magnetic field on the vacuum side of the boundary. The potential ψ has been computed previously.[1] We found that

$$\psi = -\left[\frac{a}{m}(ik_{\|}B\xi_a+iB_f)\right]\left(\frac{a}{r}\right)^m - \left[\frac{b}{m}\,iB_f\right]\left(\frac{r}{b}\right)^m.$$

The field component E_1 in the θ-z plane is given by

$$\gamma\xi_{a0}B\exp[(im\theta-ik_zz)+\gamma(t'-t)],$$

and is perpendicular to $\underline{B_0}$. Since $\underline{E_1}\times\underline{B_{1v}}$ is $\gamma\xi_aB$ times the parallel component of $\underline{B_{iv}}$, we have

$$W_{E_{11}} = \int_{-\infty}^{t}dt'\int_0^{2\pi}a\,d\theta\left(\frac{\underline{E_1}\times\underline{B_1}}{\mu_0}\right)$$

$$= \frac{1}{2\gamma}\int_0^{2\pi}a\,d\theta\,\frac{1}{\mu_0}\left[\gamma\xi_aBik_{\|}\psi\right].$$

Note that $ik_{\|}B\xi_a$ is the radial component of B_{iv}, $\frac{\partial}{\partial r}\psi \equiv \psi'$. Therefore

$$W_{E11} = \frac{1}{2\mu_0}\int_0^{2\pi} a\, d\theta\, (\psi\psi')\big|_{r=a}. \tag{7}$$

But

$$\psi\psi' = \frac{a}{m}\left[(k_{\|}B)^2 + 2(k_{\|}B)B_f\right]\xi_{a0}^2 \cos^2 m\theta$$

so that

$$W_{E11} = \frac{\pi\xi_{a0}^2}{m}\left(\frac{B_a^2}{2\mu_0}\right)\left[(m-nq_a)^2 + 2\,\frac{B_f/\xi_a}{B_a/a}\,(m-nq_a)\right]. \tag{8}$$

The feedback field B_f enters only in this term.

To compute W_{E01}, the integral of $\underline{E_1} \times \underline{B_0}$, we again find that the integral averages nearly to zero and is second-order in ξ_{a0}. There is no first-order contribution because with pressure continuity across the interface, E_1 changes sign azimuthally and as much energy drifts in as out. There is a second-order contribution, however, because of gradients in zero-order fields.

Since the gradients are in B_θ, to compute $\underline{E_1} \times \underline{B_0}$, we need E_{1z} multiplied by $\left(\underline{\xi} \cdot \underline{\frac{\partial}{\partial r}} B_\theta\right)\big|_{r=a+\xi_a}$, where $E_{1z} = (\gamma\xi_a B)(B_\theta/B)$ or $\gamma\xi_a B_\theta$, and hence

$$W_{E01} = \int_{-\infty}^{t} dt' \int_0^{2\pi} a\, d\theta\, \frac{1}{\mu_0}(\gamma\xi_a B_\theta)\left[\xi_r \frac{\partial}{\partial r} B_\theta\right]\bigg|_{r=a+\xi_a}. \tag{9}$$

Using the previous formulas for $B_\theta(r)$, we have, for $\xi_r > 0$,

$$\xi_a B_\theta\left[\xi_r \frac{\partial}{\partial r} B_\theta\right]\bigg|_{r=a+\xi_a} = -\xi_a^2 B_a^2/a,$$

and for $\xi_r < 0$

$$\xi_a B_\theta\left[\xi_r \frac{\partial}{\partial r} B_\theta\right]\bigg|_{r=a+\xi_a} = f^2\xi_a^2 B_a^2/a.$$

The integral over t' gives $1/2\gamma$, and so we have

$$W_{E01} = \frac{1}{2\mu_0}\, m\left[\int_0^{2\pi/2m} d\theta\, \xi_{a0}^2 \cos^2 m\theta\left(-B_a^2\right) + \int_{2\pi/2m}^{2\pi/m} d\theta\, \xi_{a0}^2 \cos^2 m\theta\left(f^2 B_a^2\right)\right]$$

$$= \frac{\pi\xi_{a0}^2}{m}\left[-m(1-f^2)\, B_a^2/2\mu_0\right]. \tag{10}$$

We summarize the results in terms of W_0, with

$$W_0 = (2\pi R)(\pi a^2)\left(B_a^2/2\mu_0\right)\left(\xi_{a0}^2/a^2\right)/m. \tag{11}$$

This energy is roughly $\left(\xi_{a0}^2/a^2\right)$ times the energy stored in the azimuthal magnetic field. The energy components are then

$$W_{KE} = \left(\mu_0\rho\gamma^2a^2/B_a^2\right) W_0 \tag{12}$$

$$W_{B11} = (fm-nq_a)^2 W_0 \tag{13}$$

$$W_{B01} = -2f(fm-nq_a) W_0 \tag{14}$$

$$W_{E11} = \left[(m-nq_a)^2 + 2(m-nq_a)\frac{B_f/\xi_a}{B_a/a}\right] W_0 \tag{15}$$

$$W_{E01} = -m(1-f^2) W_0. \tag{16}$$

We can write these terms more conveniently by defining

$$W_B = W_{B01} + W_{B11}$$

$$W_E = W_{E01} + W_{E11},$$

and then

$$W_B + W_E = W_{\Delta B^2} = \beta W_0, \tag{17}$$

where

$$\beta = (fm-nq_a)^2 - 2f(fm-nq_a) + (m-nq_a)^2 + 2(m-nq_a)\left(\frac{B_f/\xi_a}{B_a/a}\right) - m(1-f^2). \tag{18}$$

We set $W_{KE} + W_{\Delta B^2}$ to zero and derive the dispersion relation

$$\gamma^2 = -\beta\left(B_a^2/\rho\mu_0a^2\right). \tag{19}$$

For stability we need $\beta > 0$; therefore, in order for the kinetic energy to increase, there must be an accompanying decrease in $W_{\Delta B^2}$. Some numerical values for B_f and $W_{\Delta B^2}$ relevant to the Alcator experiment for the most unstable q_a values are as follows. For $\beta > 0$, B_f, the feedback field at $r = a$, must be

$$B_f > (k_z \xi_a)\, B_z \left\{ 1 - (m-1) \left[\frac{2(fm-nq_a) + (1-f)^2\, m}{2(m-nq_a)\, nq_a} \right] \right\}.$$

For the $m = 1$ mode, the required value of B_f is not only independent of f but also of B_a, and hence of the current I_z. This independence with respect to I_z can be traced to the increased angle between the perturbation and the field line, which provides the increased requirement on $\underline{E_1} \times \underline{B_1}$ without requiring B_f to increase. For $R = 0.5$ m and $B_z = 10^5$ G,

$$W_{\Delta B^2} = \beta W_0 \approx -(0.5/\text{m}^3) \times (\xi \text{ in cm})^2 \text{ kJ}$$

$$B_f \sim k_z B_z \xi_a \approx 2 \times (\xi \text{ in cm}) \text{ kG}.$$

Thus, we recover the dispersion relation (Eq. 19) which was obtained previously without feedback by Shafranov,[4] whose notation for f we used. We also recover the known dispersion relations for a flat current distribution (if we set $f = 1$) and for a sheet pinch (if we set $f = 0$). Further wall stabilization corrections can be obtained if we set $B_f = B_{f_{\text{wall}}}$, where

$$B_{f_{\text{wall}}} = B_a(\xi_a/a)(m-nq_a)\, \frac{(a/b)^{2m}}{1 - (a/b)^{2m}}, \tag{20}$$

which is the expression for B_f resulting from the image currents that flow naturally on a conducting wall.

The rather natural division into stored energy within the plasma plus the energy supplied to the vacuum region outside the plasma adds some clarity and insight to the physical concepts. Also, the use of Poynting flow does allow us to include an energy source in our feedback system. This is the source that complicates that part of the usual energy principle involving an integration over the vacuum region.

Our method fails, however, since we are now forced to apply the Bernstein energy principle to demonstrate that our total energy (excluding second-order fields) is conserved. The only advantage of our method is to show the difference between the small-signal energy used in the Bernstein principle and the actual energies in this problem.

To apply the Bernstein energy principle we use an intermediate form,[2] and write the change in potential energy δW (our $W_{\Delta B^2}$). We use the notation of Bernstein and his co-workers:

$$\delta W = \frac{1}{2\mu_0}\int d\tau\ |\underline{Q}|^2$$

$$-\frac{1}{2\mu_0}\int d\tau\ \mu_0\underline{j}\cdot\underline{Q}\times\underline{\xi}$$

$$-\frac{1}{2\mu_0}\int d\sigma\ (\hat{\underline{n}}\cdot\underline{\xi})\hat{\underline{B}}\cdot \text{curl}\ \underline{A}$$

$$+\frac{1}{2}\int d\sigma\ (\underline{n}\cdot\underline{\xi})^2\ \underline{n}\cdot\left\langle \text{grad}\left(p+\frac{1}{2\mu_0}\ |\underline{B}|^2\right)\right\rangle$$

$$+\frac{1}{2}\int d\tau\ \{\gamma p(\text{div}\,\underline{\xi})^2+(\text{div}\,\underline{\xi})(\underline{\xi}\cdot\text{grad}\,p)-(\underline{\xi}\cdot\text{grad}\,\phi)\,\text{div}\,(\rho\xi)\},$$

where $d\tau$ and $d\sigma$ correspond to integrations over the plasma volume and over the plasma surface, respectively, and the circumflex denotes vacuum values. Other quantities are defined in the following comments on these terms.

The first term is W_{B11}, since $\underline{Q}=\underline{B_1}$. The second term, involving the zero-order current density $\underline{j}$ is our W_{B01}, although the correspondence is not as obvious as for the first term. The difference in viewpoint is that here $(\underline{j}\times\underline{Q})\cdot\underline{\xi}$ is a $J\times B$ force $\times$ a distance while our $\underline{2B_1}\cdot\underline{B_0}/2\mu_0$ is the resultant energy change after the displacement. We get the same result in both cases. That is, for $k_za \ll 1$, $\underline{j}$ and $\underline{Q}\times\underline{\xi}$ are essentially parallel everywhere; $|\mu_0\underline{j}|$ is $2B_\theta/r$ or $2fB_a/a$; $|\underline{Q}\times\underline{\xi}|$ is $k_{||}B\xi^2$ or $(B_a/a)(fm-nq_a)\cdot\xi_{a0}^2(r/a)^{2m-2}$. Thus the term $\underline{j}\cdot\underline{Q}\times\underline{\xi}$ is $(-2f)/(fm-nq_a)\times$ the first term, as we have already found.

The third term is our term W_{E11}. Here, $\nabla\times\underline{A}$ is our B_{1v} in the vacuum region and $(\underline{n}\cdot\underline{\xi})\hat{\underline{B}}/2\mu_0$ is our $E_1/2\gamma\mu_0$. Since E_1 is perpendicular to the zero-order field $\underline{\hat{B}_0}$, the angle between $\underline{E_1}$ and $\underline{B_1}$ is complementary to the angle between $\underline{B_1}$ and $\underline{\hat{B}_0}$; and so the sine of the angle in the vector product $\underline{E_1}\times\underline{B_1}$ is the same as the cosine of the angle in $\underline{B_1}$'s dot product with $\underline{\hat{B}_0}$. Alternatively, we could note that $(\underline{n}\cdot\underline{\xi})\hat{\underline{B}}\cdot\nabla\times A$ goes to $(\underline{n}\cdot\underline{\xi})\hat{B}ik_{||}\psi$ (with $\nabla\times\underline{A}=\nabla\psi$), and, by the field-freezing condition, $(\underline{n}\cdot\underline{\xi})ik_{||}\hat{B}$ is $B_{r1}=\frac{\partial}{\partial r}\psi\equiv\psi'$. Thus this third term becomes $(1/2\mu_0)\int d\sigma\ \psi\psi'$, which is just our integral.

The fourth term is our term W_{E01}. Here $\left\langle \text{grad}\left(p+\frac{|\underline{B}|^2}{2\mu_0}\right)\right\rangle$ is the jump in grad $\left(p+B_\theta^2/2\mu_0\right)$ across the boundary. For the current considered here (constant current density + a sheet current at r = a), the equilibrium pressure is

$$p = \begin{cases} (1-f^2)B_a^2/2\mu_0 + \left(f^2B_a^2/2\mu_0\right)(1-(r/a)^2) & r < a \\ 0 & r > a \end{cases}$$

and

$$\frac{B_\theta^2}{2\mu_0} = \begin{cases} f^2B_a^2(r/a)^2/2\mu_0 & r < a \\ B_a^2(a/r)^2/a\mu_0 & r > a \end{cases}$$

Hence

$$\left\langle \text{grad}\left(p+B_\theta^2/2\mu_0\right)\right\rangle = -\left(\frac{B_a^2}{a\mu_0}\right) - \left[-2\frac{f^2B_a^2}{a\mu_0} + \frac{f^2B_a^2}{a\mu_0}\right]$$

$$= -(1-f^2)\left(B_a^2/a\mu_0\right). \tag{21}$$

Thus, the fourth term is $\int_0^{2\pi} a\,d\theta\,\xi_{a0}^2 \cos^2 m\theta(1-f^2)\left(-B_a^2/2a\mu_0\right)$ which gives our result, $(1-f^2)\left(-\pi\xi_{a0}^2B_a^2\right)/2\mu_0$.

The last term drops out because there is no ϕ (ϕ is the external potential energy, for example, gravity) and we have taken $(\nabla\cdot\underline{\xi})$ to be zero.

This correspondence between our formulation and the Bernstein result does not resolve our initial question of second-order forces. We were not attempting to compute a small-signal energy in terms of first-order quantities but rather the total change in system energy. We have not yet demonstrated whether the terms with $\underline{E_2} \times \underline{B_0}$ and $\underline{B_2}\cdot\underline{B_0}$ are third-order in ξ_{a0} when volume-averaged, or whether they are second-order and negligible, or second-order and should be included.

In the last case we can claim that their sum is zero by invoking our conservation statement for the sum of the seven original terms, together with the conservation of the terms in the Bernstein conservation statement.

Wall Effects

A conducting wall at r = b provides some feedback stabilization. If the wall resistivity η is zero, the flow of image currents on the wall keeps the perturbed radial field at the wall zero. These currents produce the feedback field of Eq. 20. Using this value, we find that the dispersion relation is

$$\gamma^2 = -\beta_0\left(B_a^2/\rho\mu_0 a^2\right),$$

where

$$\beta_0 = (fm-nq_a)^2 - 2f(fm-nq_a) + (m-nq_a)^2 \frac{(a/b)^{2m}}{1-(a/b)^{2m}} - m(1-f^2). \tag{22}$$

Next, we assume that the walls have a small but finite resistivity. Unstable modes are not significantly affected by finite η but the otherwise stable propagating modes will damp at a rate $(-\gamma_\eta)$, where for these propagating modes we let $\gamma = \gamma_\eta - i\omega$. For $\eta = 0$, these modes are characterized by $\beta_0 > 0$ and $\omega = \omega_0 \neq 0$, where β_0 and ω_0 are the $\eta = 0$ values of β and ω. For $\eta = 0$, damping occurs because of the "$R/\omega L$" phase lag of the image currents with respect to the propagating plasma wave. This phase lag, $1/\omega\tau$ (where τ is the "L/R" time for these image currents on a wall at $r = b$ outside a perfect conductor at $r = a$) is given by

$$\frac{1}{\omega\tau} = \frac{1}{\omega}\left[\frac{\eta}{\delta}\left(\frac{m/b}{\mu_0}\right)\frac{2}{1-(a/b)^{2m}}\right], \tag{23}$$

with δ the skin depth. For small η, B_f and β have essentially the $\eta = 0$ magnitudes, $B_{f,\eta=0}$ and β_0, but the phase lag gives them, a small imaginary part. That is,

$$B_f = B_{f,\eta=0}\left[1 - i\frac{1}{\omega\tau}\right]$$

and

$$\beta = \beta_0\left[1 - i\frac{1}{\omega\tau}(m-nq_a)^2\frac{2(a/b)^{2m}}{1-(a/b)^{2m}}\right]. \tag{24}$$

Using this β in $\gamma^2 = -\beta\left[\frac{B_a^2}{\rho\mu_0 a^2}\right]$ and noting that $\omega \approx \omega_0$, we obtain γ_η from the imaginary part of this equation

$$\gamma_\eta = -\frac{1}{2\beta_0}\left[\frac{\eta}{\delta}\left(\frac{m/b}{\mu_0}\right)\left(\frac{2(a/b)^m}{1-(a/b)^{2m}}\right)^2\right]. \tag{25}$$

For (η/δ) of 10^{-4} Ω (corresponding to the resistivity of copper and 10^5 Hz frequencies) and for $b = 0.2$ m, the damping time γ_η^{-1} is

$$\gamma_\eta^{-1} = \frac{\mu_0 b}{2(\eta/\delta)} \frac{1}{m} \left[\left(\frac{b}{a}\right)^m - \left(\frac{a}{b}\right)^m\right]^2 \beta_0$$

$$\approx 10^{-3} \frac{1}{m} \left[\left(\frac{b}{a}\right)^m - \left(\frac{a}{b}\right)^m\right]^2 \beta_0 \text{ seconds.}$$

Thus, the damping time is milliseconds for low m number modes (for $(b/a)^{2m}/m \sim 1$) having $\beta_0 \sim 1$. (That is, for modes that are within a few wavelengths of the wall and that are not too far from marginal stability.)

Resistive growth rather than damping can occur if the plasma has a zero-order rotation, such as may be induced by a radial electric field, as has been examined recently by Rutherford, et al.[5] Growth occurs when the phase velocity between B_f and the plasma wave changes sign. This sign change occurs if the rotation is opposite to and faster than the phase velocity. Then the phase lag of B_f along the wall is a phase lead as viewed from the plasma, and this lead produces growth.

We have also examined this problem in terms of energy. Since we know the magnitude of the image currents on the wall, we can compute the rate of wall heating caused by these currents. This heating rate equals the rate at which wave energy decreases. This decrease represents damping if the wave energy is positive and growth if the wave energy is negative.

The wave energy depends on the frame of reference. In the frame of the wall the component W_{KE} of the wave energy picks up an additional contribution when rotation is added. There is now a zero-order velocity v_0 so that in addition to ρv_1^2 we have a contribution from $\rho v_0 v_1$, which can be a positive or negative contribution, depending on whether the wave induces a net increase or a net decrease in the kinetic energy stored in rotation. By including this term, we can show that the kink modes are action conserving, where action is defined as the observed wave energy divided by the observed wave frequency. Thus, for modes whose phase velocity has been reversed in direction by the rotation, the wave energy is negative.

Thus growth is expected from the viewpoint of energy conservation too. For modest rotational speeds, it is the modes near marginal stability whose phase velocity might be reversed by the rotation, since their phase velocity relative to the plasma is small. From either calculation, we obtain the growth rate

$$\gamma_\eta = \left(\gamma_{\eta, v_{\theta 0}=0}\right) \Bigg/ \left[1 + \frac{v_{\theta 0}}{\left(\frac{m}{a}\right)\sqrt{\beta_0 B_a^2/\rho\mu_0 a^2}}\right], \tag{26}$$

where $\gamma_{\eta, v_{\theta 0}=0}$ is the value derived for no rotation, and $v_{\theta 0}$ is the azimuthal rotational velocity at r = a.

R. S. Lowder, K. I. Thomassen

References

1. R. S. Lowder and K. I. Thomassen, Quarterly Progress Report No. 101, Research Laboratory of Electronics, M.I.T., April 15, 1971, pp. 81-87; Quarterly Progress Report No. 102, July 15, 1971, pp. 93-96.

2. I. Bernstein, E. A. Frieman, M. D. Kruskal, and R. Kulsrud, Proc. Roy. Soc. (London) A244, 17-40 (1958).

3. V. D. Shafranov, Zh. Tekh. Fiz. 40, 241 (1970); Soviet Phys. – Tech. Phys. 15, 175 (1970).

4. V. D. Shafranov, in Plasma Physics and the Problem of Controlled Thermonuclear Reactions, Vol. IV, M. A. Leontovich (Ed.), translated from Russian by J. Turkovich (Pergamon Press, New York, 1959), p. 71.

5. P. H. Rutherford, H. P. Furth, and M. N. Rosenbluth, Paper CN28/F-16, presented at the Fourth Conference on Plasma Physics and Controlled Nuclear Fusion Research, Madison, Wisconsin, June 1971.

XIII. PLASMAS AND CONTROLLED NUCLEAR FUSION*

F. High-Temperature Plasma Physics

Academic and Research Staff

Prof. B. Coppi
Dr. D. B. Montgomery†
Prof. G. Bekefi
Prof. A. Bers
Prof. R. A. Blanken
Prof. R. J. Briggs
Prof. L. M. Lidsky
Prof. R. R. Parker
Prof. K. I. Thomassen
Dr. E. Minardi
Dr. L. Ornstein
Dr. P. A. Politzer
Dr. J. Rem
Dr. D. Schram
Dr. F. C. Schüller
Dr. D. J. Sigmar
A. Hugenholtz

Graduate Students

E. L. Bernstein
D. L. Cook
R. Dagazian
D. P. Hutchinson
Y. Y. Lau
M. A. Lecomte
A. R. Millner
M. Simonutti
N. R. Southoff
B. V. Waddell
D. C. Watson

RESEARCH OBJECTIVES

The physics of high-temperature plasmas is of primary importance in the problem of controlled thermonuclear fusion and to astrophysics in general. The main point of interest for the controlled thermonuclear program is the production and magnetic confinement of dense plasmas ($n \gtrsim 10^{14}$ particles/cm^3) with thermal energies in excess of 5 keV. On the other hand, important astrophysical questions related to the understanding of high-temperature plasma dynamics are the nature of thermal and nonthermal radiation mechanisms from the magnetosphere of collapsed stars (x-ray stars and pulsars are thought to be associated with this class), the development of solar flares, and so forth.

Considerable experimental and theoretical effort has been undertaken in order to understand the dynamics of plasmas in the regimes mentioned above, and in particular their transport properties. In fact, it is recognized that in conditions wherein the two-body collision mean-free paths are very long the transport coefficients of a plasma are determined, for the most part, by the collective modes that are excited in it rather than by two-body collisions.

In magnetically confined plasmas at high temperatures two classes of particles may be distinguished: particles that are trapped in the local wells of the inhomogeneous magnetic field and circulating particles that sample the entire length of the lines of force. As a result, new collective modes can be generated and have an important effect on the stability and transport properties of the plasma that is being considered.

To investigate these and other aspects, a sequence of experimental apparatus is being put into operation, in particular, a linear quadrupole that is the simplest two-dimensional configuration for the study of trapped-particle dynamics, and a relatively large toroidal configuration (Alcator) designed to achieve new plasma regimes and to analyze new methods of plasma heating. A more advanced toroidal configuration capable of sustaining high plasma currents is in the design stage.

*This work was supported by the U.S. Atomic Energy Commission (Contract AT(11-1)-3070).

†Dr. D. Bruce Montgomery is at the Francis Bitter National Magnet Laboratory.

A special experimental program is being organized to investigate the x-ray, optical, and infrared emission from Alcator. This is in view of its astrophysical implications and of the importance that radiation has in the energetic balance of thermonuclear plasmas.

B. Coppi